

Journal of Materials Chemistry B

Accepted Manuscript



This is an *Accepted Manuscript*, which has been through the Royal Society of Chemistry peer review process and has been accepted for publication.

Accepted Manuscripts are published online shortly after acceptance, before technical editing, formatting and proof reading. Using this free service, authors can make their results available to the community, in citable form, before we publish the edited article. We will replace this *Accepted Manuscript* with the edited and formatted *Advance Article* as soon as it is available.

You can find more information about *Accepted Manuscripts* in the [Information for Authors](#).

Please note that technical editing may introduce minor changes to the text and/or graphics, which may alter content. The journal's standard [Terms & Conditions](#) and the [Ethical guidelines](#) still apply. In no event shall the Royal Society of Chemistry be held responsible for any errors or omissions in this *Accepted Manuscript* or any consequences arising from the use of any information it contains.



6 Nerve Conduit Constructed by Electrospun P(LLA)CL Nanofiber 7 and PLLA Nanofiber Yarn

1 Received 00th January 20xx,
2 Accepted 00th January 20xx

3 DOI: 10.1039/x0xx00000x

4 www.rsc.org/

8 Dawei Li^{a, b}, Xin Pan^b, Binbin Sun^b, Tong Wu^b, Weiming Chen^b, Chen Huang^a, Qinfei Ke^{a, c}, Hany A
9 El-Hamshary^{d, e}, Salem S Al-Deyab^d, Xiumei Mo^{a, b*}

10 Injuries of peripheral nerve occur commonly in various people of different ages and backgrounds. Generally, surgical
11 repairing such as suturing the transected nerve stumps and transplanting autologous nerve graft is the only choice.
12 However, tissue engineering provides an alternative strategy for regeneration of neural context. Functional nerve conduits
13 with three dimensional (3D) support and guidance structure are badly in need. Herein, uniform PLLA nanofiber yarn
14 constructed by unidirectionally aligned nanofiber was fabricated via dual spinneret system. Which was subsequently
15 incorporated into a hollow poly(L-lactide-co-caprolactone) (P(LLA-CL)) tube to form a nerve conduit with inner aligned
16 texture. The biocompatibility of poly(L-lactic acid) (PLLA) yarn was assessed by in vitro experiments. Schwann cells (SCs)
17 presented better proliferation rate and spread morphology on PLLA yarn than that of PLLA film. Confocal images indicated
18 the axon spread along the length of yarn. SCs were also cultured in the conduit. The data indicated that SCs proliferated
19 well in the conduit and distributed dispersedly throughout the entire lumen. These results demonstrated the potential of
20 PLLA nanofiber yarn conduit in nerve regeneration.

21 Introduction

22 Peripheral nerve injury is a common global problem
23 occurs to people of different backgrounds, which often
24 leads to the loss of sensory and motor function. Various
25 methods were invented to repair the nerve injury.
26 Surgically, short nerve lesion can be appropriately
27 repaired by end to end coaptation. However, for the long
28 distance nerve defection, end to end anastomosis is no
29 longer an option for it causes detrimental tension along
30 the nerves and retards healing¹. In these cases, a graft is
31 needed to bridge the nerve gap and provide better
32 regenerative outcomes. Currently, autologous nerve
33 grafts are considered as the “gold standard” for gap
34 injuries greater than 5-10 mm². However, some
35 drawbacks restrict its application, such as limited donor
36 resource, sacrifice of the donor, extra incision, and
37 possible size mismatch. Customized grafts for specific
38 nerve injuries are desired for better cure with little side

39 effect and additional sacrifice.

40 The progress of tissue engineering scaffold provides a
41 promising alternative for nerve repair. Nerve conduits
42 can act as a bridge between adjacent ends, providing
43 directional guidance and biological support during nerve
44 regeneration. To better adjust the interaction of cells,
45 tissue, and the conduit, scaffolds with nanoscale
46 topology are extensively introduced to the manufacture
47 of nerve scaffolds. Diverse fabrication methods have
48 been used to prepare nanostructured scaffolds, such as
49 phase separation^{3, 4}, self-assembly⁵, as well as
50 electrospinning⁶⁻⁸. The most commonly used designs
51 include the hollow tubes (Fig. 1 (a)), multiple channels
52 conduits (Fig. 1 (b)), tube filled with internal matrix with
53 longitudinal oriented channels or pore (Fig. 1 (c))⁹⁻¹², as
54 well as lumen filled with aligned polymer fibers as
55 longitudinal guidance (Fig. 1 (d), (e))^{8, 13-21}.

56 Electrospinning is mostly reported due to its easy
57 handleability, cost efficiency, quality controllability, and
58 availability for various natural and synthetic materials.
59 Electrospun nanofiber scaffolds can mimic the basic
60 nanoscale structure of natural extracellular matrix.
61 Parallel fibers have demonstrate the ability to guide the
62 spreading and migration of Schwann cells (SCs)^{8, 22-24}.
63 Additionally, aligned fibers may induce the
64 differentiation and maturation of neural stem cells and
65 SCs^{25, 26}. Dorsal root ganglia (DRG) cultured on the

^aEngineering Research Center of Technical Textiles, College of Textiles, Donghua University, Shanghai 201620, China. E-mail: xmm@dhu.edu.cn; kjf@dhu.edu.cn

^bState Key Lab for modification of chemical fibers & polymer materials, College of Chemistry, Chemical Engineering and Biotechnology, Donghua University, Shanghai, 201620, China.

^cShanghai Normal University, Shanghai, 200234, China.

^dDepartment of Chemistry, College of Science, King Saud University, Riyadh, Kingdom of Saudi Arabia

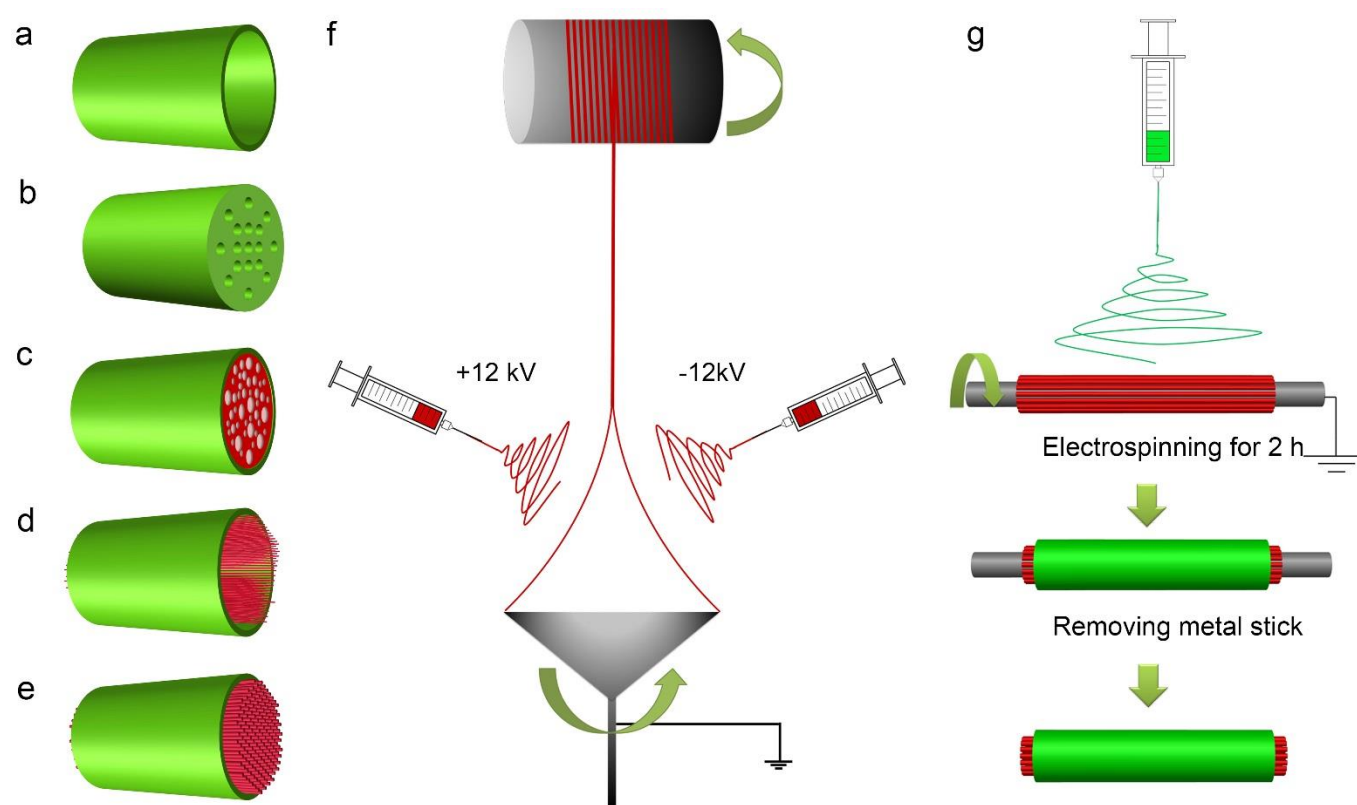
^eDepartment of Chemistry, Faculty of Science, Tanta University, Tanta, Egypt

1 parallel nanofiber tended to generate long and
2 unidirectionally ordered neurites. The predetermined
3 aligned nanofiber could cause SC alignment and
4 subsequent neurite extension in vitro. Studies also
5 have shown the unidirectional electrospun nanofiber,
6 but not the randomly oriented nanofiber, could guide
7 nerve regeneration across long nerve gaps¹⁹. However,
8 the traditional electrospinning process always
9 manufactured 2D film with densely compacted
10 structure which inhibited cell infiltration and
11 immigration into the scaffold²⁷. Andreas Kriebel et al
12 have tried v-shaped collector to collect aligned
13 nanofibers with 3D structure which was subsequently
14 incorporated into collagen matrix²¹. While the guiding
15 function of parallel nanofiber was struck for axons also
16 adhere to the surrounding hydrogel. Several types of
17 nerve conduits have been designed to incorporate
18 aligned electrospun nanofiber in the internal of the tube.
19 The most commonly used method is to fabricate tubes
20 with axially aligned nanofibers constructing the inner
21 surface of the tube^{23, 28, 29}. Jingwei Xie et al. fabricated
22 double layered nerve conduits with the aligned PCL
23 nanofiber as the inner surface while the random fiber
24 served as the supporting wall²³. In vivo results indicated
25 that the bilayer conduits could effectively improve nerve
26 fiber sprouting and motor recovery. This approach could
27 facilitate cell spreading and migration but did not
28 provide effective support for cell growth in the space of
29 the lumen. Eric M Jeffries et al. reported 3D multichannel
30 nerve conduit incorporated with parallel electrospun
31 fibers¹⁸. This guide had thin walls and high channel
32 numbers to maximize surface area and facilitated cell
33 spreading and migration. However, the manufacturing
34 process was labor intensive and varied by operator,
35 which limited the effective conduit length and
36 reproducibility. Another commonly used method is to
37 insert a bundle of aligned nanofibers in the nerve guide^{15,}
38 ^{17, 19-21}. Highly aligned nanofiber film was cut into thin
39 strips and incorporated in a hollow nerve conduit by
40 Young-tae Kim et al¹⁹. The presence of aligned nanofiber
41 film could maximize the topographic directional cues for
42 neurite outgrowth and SCs migration in 3D configuration.
43 However, the width of the stripes may also lead to
44 unevenness of tissue regeneration in the sectional

45 direction. 3D scaffold consisting parallel fibers were
46 fabricated via modulating the collector by Andreas
47 Kriebel et al²¹ and Balendu S. Jha et al¹⁵. Both studies
48 demonstrate the parallel fibers could direct axonal
49 regeneration and SCs migration along a defined axis.
50 Nevertheless, the scaffolds constructed by parallel fibers
51 were quite soft and difficult to handle. Moreover the
52 densely packed nanofibers may inhibit cell infiltration^{21,}
53 ²⁷.

54 In this study, a novel approach is introduced to
55 manufacture long distance nerve conduits with aligned
56 electrospun nanofiber as the filler and randomly
57 electrospun nanofiber as the shell. Our method is based
58 on the fabrication of nanofiber yarn by a dual spinneret
59 electrospinning system. Yarn constructed by nanofiber
60 inherits various features of nanofiber, but also possessed
61 unique properties such as easy post-processing.
62 Nanofiber yarn can be manufactured by textile and
63 related methods into a fabric and other predetermined
64 structure. Various techniques were introduced to
65 fabricated nanofiber yarn. Ko et al. firstly electrospun
66 continuous nanoscale composite yarn with a complex
67 setup with orientation, twisting, and take up
68 components³⁰. Smit et al. drawn the electrospun
69 nanofiber web from the water bath and collected
70 continuous yarns³¹. Teo et al. used the water vertex
71 while water flowing from the hole of a basin to generate
72 continuous nanoscale yarn³². A grounded tip was applied
73 to induce self-bundling nanofiber yarn by Wang et al³³.
74 Recently, nanofiber yarn was fabricated by the
75 oppositely charged dual nozzle system³⁴⁻³⁶. In which, the
76 nanofiber yarn could be twisted and collected at the
77 same time.

78 Herein, PLLA nanofiber yarn was fabricated use the dual
79 nozzle electrospinning system. The random nanofibers
80 electrospun from P(LLA-CL) solution possess excellent
81 mechanical properties for the nerve conduits and
82 provide the conduit tear-resistant during surgical
83 procedure. Whereas the highly aligned nanofiber in the
84 nanofiber yarn made of PLLA serve as the guidance for
85 axons spreading and cell migration. Characterization of
86 the PLLA nanofiber yarn and nerve conduit was
87 conducted, while SCs was cultured on the PLLA nanofiber
88 yarn and in the nerve conduits to study the biological
89 performance.



90

91

92 Fig. 1 Schematic of various conduits: (a) hollow lumen conduit, (b) multichannel conduit, (c) sponge-containing conduit, (d)
 93 fiber-containing conduit, and (e) nanofiber yarn-containing conduit. (f) The mechanism of nanofiber yarn fabrication. (g)
 94 Schematic of incorporating nanofiber yarn into the conduit.

95

96 2. Materials and experiments

97 2.1 Materials

98 PLLA with an average molecular weight (M_w) of 500 kDa
 99 was purchased from Daigang Biomaterials Inc. (Jinan,
 100 China). P(LLA-CL) ($M_w=300$ kDa, LA:CL=50:50) was
 101 supplied by Nara Medical University, Japan.
 102 Hexafluoroisopropanol (HFIP) was obtained from
 103 Shanghai Darui Finechemical Co., Ltd. (China). The
 104 Dulbecco's Modified Eagle's Medium (DMEM, Hyclone),
 105 fetal bovine serum (FBS, Gibico), trypsin (Hyclone) 3-(4,

106 5-dimethylthiazol-2-yl)-2, 5-diphenyltetrazoliumbromide
 107 (MTT, Sigma) was purchased from Yuanzhi Biotechnology
 108 Co., Ltd (Shanghai, China). 4', 6-Diamidino-2-
 109 phenylindole (DAPI) and Alexa Fluor® 568 phalloidin was
 110 supplied by Life Technologies Co., Ltd. (USA).

111 2.2 Preparation of PLLA nanofiber yarn

112 0.75 g PLLA was dissolved in 10 mL HFIP to generate
 113 7.5% w/v PLLA solution. The nanofiber yarn was
 114 fabricated by a dual spinneret electrospinning system as
 115 described by Usman Ali et al.³⁶. As illustrated in Fig. 1 (f),

1 the setup consists of two spinneret, a plastic funnel
2 (diameter=10 mm) with conductive edge which was
3 grounded, a yarn winder (diameter 8 mm), and two high
4 voltage DC power supplies (Gamma High Voltage
5 Research, USA). During electrospinning, the PLLA
6 solution was added in the two oppositely positioned
7 syringes and squeezed out through the metal needles of
8 20 gauge. The flow rate of PLLA solution was set at 1.0
9 mL/h. Two needles were separately charged with
10 positive (+ 12 kV) and negative (-12 kV) high voltage.
11 Electrospun nanofibers from two nozzles were deposited
12 on the rotary funnel and covered the funnel end with a
13 nanofiber layer. A cone shaped nanofiber layer could
14 form on the funnel edge by initial inducing. After drawing
15 by the winder and twisting by the rotary funnel, a
16 continuous nanofiber yarn was obtained. As a control,
17 PLLA nanofiber film was prepared by a single
18 electrospinning nozzle and collected on aluminum foil.
19 The voltage, spinning rate, and collecting distance was
20 set as +12 kV, 1.0 mL/h, and 15 cm, respectively.

21 2.3 Characterization

22 The surface of nanofiber yarn was sputter-coated with
23 gold and subsequently observed by a Digital Vacuum
24 Scanning Electron Microscope (SEM, TM 3000, Hitachi,
25 Japan) at the accelerating voltage of 15 kV. Diameter of
26 fibers in the nanofiber yarn was measured on the SEM
27 images by the image visualization software Image J
28 (National Institutes of Health, USA). 100 fibers were
29 randomly selected for each sample.

30 2.4 In vitro experiments

31 SCs were maintained and expanded in DMEM culture medium,
32 incubated in humidified atmosphere with 5% CO₂ at 37 °C.
33 The culture medium was refreshed every other day. For in
34 vitro biocompatibility assessment, the PLLA nanofiber yarn
35 was wound on a square glass slip (a side of 10 mm) till the
36 entire surface was covered by the yarn. The PLLA film was cut
37 into round pieces with a diameter of 15 mm. The samples
38 were fixed in the 24-well culture plates by stainless steel rings
39 with an inner diameter of 10 mm. Subsequently, the plates
40 were sterilized by alcohol steam in sealed desiccator for 48 h.
41 Scaffolds in the plate were rinsed with phosphate-buffered
42 saline solution (PBS) for 3 times and washed with culture
43 medium for 1 time.

44 2.5 Adhesion and proliferation of SCs

45 For the assessment of SCs adhesion on the PLLA nanofiber
46 yarn, a total number of 4×10⁴ cells were seeded on the
47 scaffolds in 24-well plate to compare the cell adhesion PLLA
48 nanofiber yarn and film with tissue culture plates (TCPs) as
49 control. 40 min, 60 min, 120 min and 240 min after seeding,
50 the culture medium was removed and the specimens were

51 rinsed with PBS 3 times to remove the unattached and dead
52 cells. Then, the amount of the attached cells was determined
53 by standard MTT assay. Briefly, the specimens were
54 incubated in 360 μL FBS-free DMEM culture medium and 40
55 μL 5 mg mL⁻¹ MTT solution for 4 h. Thereafter, the culture
56 media were pipetted out and 400 μL dimethylsulfoxide
57 (DMSO) was added. Afterwards, the plate was incubated in a
58 shaker at 37 °C for 30 min. While the crystal was thoroughly
59 dissolved, 100 μL of the solution was transferred to a 96-well
60 plate and tested by a microtiter plate reader (Multiskan MK3,
61 Thermo, USA), at the absorbance of 492 nm.

62 For proliferation study, 1×10⁴ cells were seeded on the
63 scaffolds with TCP as control. The amount of the cells on each
64 specimen was determined by the standard MTT assay. 1, 3,
65 and 7 days post seeding, the culture medium was removed
66 and unattached cells were washed away with PBS for three
67 times, MTT assay was conducted as described above to
68 determine the amount of viable cells on the scaffolds. For
69 each group 6 specimens were tested.

70 2.6 Cell morphology observation

71 A total number of 1.0×10⁴ cells were seeded on the nanofiber
72 yarn and film in 24-well plates. After culturing for 1, 3, 7 days,
73 cells cultured on the scaffolds were fixed by 4%
74 paraformaldehyde for 2 h min at 4 °C, dehydrated with
75 gradient ethanol solution (30%, 50%, 70%, 90%, 95%, and
76 100%) and followed by freeze drying at -60 °C for 12 h.
77 Afterwards, the samples were sputter coated with gold and
78 observed by SEM at the accelerating voltage of 15 kV.

79 Confocal laser scanning microscopy (CLSM, Carl Zeiss, LSM
80 700, Germany) was used to visualize the morphology and
81 distribution of cells on the scaffolds. After 1, 3, 7 days of
82 culture, the specimens with cells were rinsed twice with PBS
83 and then fixed with 4% paraformaldehyde for 2 h min at 4 °C.
84 Subsequently, the cells on the scaffolds were permeabilized
85 by 0.1% Triton X-100 (Sigma, USA) for 10 min. After rinsing 3
86 times with PBS, the cytoskeletons and nuclei of cells were
87 stained with 25 μg/mL rhodamine-conjugated phalloidin and
88 10 μg/mL DAPI for 30 min and 5 min, respectively.
89 Subsequently, the cells were visualized using CLSM.

90 2.7 Fabrication of nerve conduit

91 The schematic of fabrication of nerve conduit was illustrated
92 in Fig. 1 g. Briefly, 1.2 g P(LLA-CL) was dissolved in 10 mL HFIP
93 to generate 12% w/v P(LLA-CL) solution, which was
94 subsequently applied in single spinneret electrospinning. The
95 applied voltage, electrospinning distance and flow rate were
96 controlled at 12 kV, 15 cm, and 1.5 mL/h, respectively. The
97 as-prepared PLLA nanofiber yarns (red in Fig. 1 (g), effective
98 length of 6 cm) were parallelly fixed around the metal stick
99 (grey in Fig. 1 (g), diameter of 2.5 mm) along the axis of the

1 stick. The stick was fixed on a motor with a rotating rate of 5
2 rpm and grounded to collect the electrospun P(LLA-CL)
3 nanofiber (green in Fig. 1 (g)). The electrospinning lasted for
4 two hours. Finally, the metal stick was removed and the
5 conduit was well prepared. The nerve conduit was incubated
6 in vacuum oven for 48 h to remove the residual solvent.

7 2.8 In vitro cell culture

8 To test the biocompatibility of the nerve conduit, the as-
9 prepared conduit was cut into short sections with a length of
10 9 mm. SCs was co-cultured with the conduit sections. The
11 ethanol steam sterilized conduit section was placed in wells
12 of 24-well plate. After washed with PBS and culture medium,
13 500 μ L of cell solution of 4×10^5 cells/mL was pipetted into the
14 end of each section of nerve conduit. Afterwards, the conduit
15 sections were let lied in the culture plate and incubated on a
16 shaker (60 rpm) in the incubator. The culture medium was
17 refreshed every other day. After 1, 3, 7 days of culture, the
18 conduit section combined with cells was transferred into a
19 new plate. MTT assay was conducted as described above to
20 determine the amount of viable cells in the conduit.

21 2.9 Cell proliferation and migration in the nerve conduit

22 To observe the distribution of cells in the conduit, conduits
23 combined with SCs was fixed after 7 days of culture with 4%
24 paraformaldehyde for 2 h min at 4 °C. The samples were
25 embedded in sample freezing medium and plunge frozen at -
26 80 °C. The frozen samples were sliced into thin slices with a
27 thickness of 30 μ m at -40 °C. Cross sections in axial direction
28 were obtained. Slices were collected on glass slides and
29 stained with DAPI, followed by observed with CLSM.

30 2.10 Statistical analysis

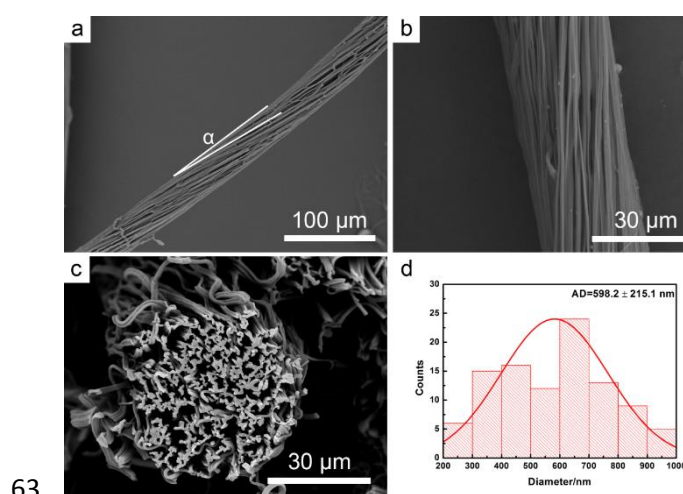
31 All the data were obtained at least in triplicate and all values
32 were presented as the mean and standard deviation (SD).
33 Statistical analysis was performed by the one-way analysis of
34 variance using Origin 8.0 (OriginLab Inc., USA). The statistical
35 difference between two sets of data was considered when *
36 $p < 0.05$ and ** $p < 0.01$.

37 Results and discussion

38 3.1 Electrospun nanofiber yarn

40 Dual spinner etelectrospinning was conducted to
41 fabricated PLLA nanofiber yarn with highly aligned
42 nanofiber. The schematic of yarn fabrication is
43 illustrated in Fig. 1 (f) and the SEM images of nanofiber
44 yarn were shown in Fig 2. It can be seen that PLLA
45 nanofibers in the surface of the nanofiber yarn were
46 unidirectionally oriented along the axis of the yarn

47 body within a tiny twisting angle α ($8.37 \pm 1.69^\circ$, Fig.
48 2 (a), (b)). Ali Usman et al reported that increasing the
49 rotating speed of the metal funnel could rise the
50 twisting angle and meanwhile strengthen the
51 mechanical property³⁶. Herein, we chose a low funnel
52 rotating speed of 300 rpm to minimize the twisting
53 angle and got nanofibers aligned to the axis of the yarn.
54 The cross-section of the nanofiber yarn was illustrated
55 in Fig. 2 (c). Two or three fibers combined into a bundle
56 with grooves forming between adjacent fibers. Porosity
57 could still be observed in the yarn, which could
58 increase the specific surface area and thus facilitate the
59 transport of nutrition and degradation. The average
60 diameter of the PLLA nanofibers in the yarn was 598.2
61 ± 215.1 nm (Fig. 2 (d)). The average diameter of the
62 PLLA yarn was 49.7 ± 14.6 μ m.



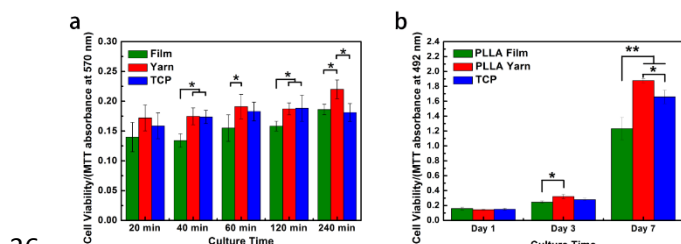
63
64 Fig. 2 SEM images of the nanofiber yarn. Morphology of
65 the surface of PLLA nanofiber yarn (a), (b). Cross
66 section of the nanofiber yarn (c). Diameter distribution
67 of PLLA nanofiber in the nanofiber yarn (d).

68 3.2 SC adhesion and proliferation

69 Cell adhesion on PLLA nanofiber yarn and film was
70 assessed by determining the amount of viable SCs
71 attached to each scaffold with MTT assay. According to
72 our previous research, most SCs could attach to
73 scaffolds in about 4 hours. Thus the time period for cell
74 adhesion was set as 240 min. As illustrated in Fig 3 (a),
75 cells attach to the PLLA nanofiber film kept the least in
76 240-min culture period. After 240 min of incubation,
77 SCs on the nanofiber yarn are significantly more than
78 that of TCP. MTT analysis shows that nanofiber yarn
79 had better cell adhesion capacity than nanofiber film,
80 which might further benefit the spreading and
81 proliferation of cells on the scaffold. Nanofiber is

1 believed that the nanoscale topology and high specific
2 surface area could mimic the natural extracellular
3 matrix (ECM) and facilitate cell growth and tissue
4 regeneration. However, nanofibrous structure also
5 reduces the pore size of the scaffold, inhibiting cells on
6 the very surface and hindering cell migration into the
7 scaffold. The nanofiber yarn can provide fluctuant
8 surface of microscope, which increases the effective
9 surface for cell adhering. Thus, more cells can attach to
10 the scaffold in the initial several hours, enhancing the
11 adhesion of SCs.

12 Longer period culturing was conducted to study the
13 proliferation of SCs on the nanofiber yarn. MTT assay
14 was conducted after 1, 3, 7 days of culture to
15 determine the amount of viable cells. As shown in Fig. 3
16 (b), during 7 days of culture, SCs go through remarkable
17 increase on three groups of substrates, implying that
18 the PLLA nanofiber scaffolds can support the
19 proliferation of SCs. 3 days post-seeding, more SCs are
20 detected on the PLLA nanofiber yarn than film. The
21 difference is enlarged over time. 7 days later, amount
22 of SCs on the nanofiber yarn even surpasses that on
23 TCP. It can be obviously concluded that the PLLA
24 nanofiber yarn could significantly enhance SCs
25 proliferation. As mentioned above, the microscope
26 structure of nanofiber yarn can provide more space for
27 cell spreading and migration. As shown in Fig. 4 (f), SCs
28 covers the whole surface of the yarn, including the
29 upper side, lateral sides, and even the underside.
30 However, restricted by the small pores between the
31 nanofibers, the film possesses no extra space for cell
32 growth except the upper surface. In addition, the
33 micro-structure of the yarn also facilitates the transport
34 of nutrition and metabolic waste, which also
35 contributes to the cell proliferation.



37 Fig. 3 Analysis of MTT assay for SCs adhesion (a) and
38 proliferation (b) on PLLA film, PLLA nanofiber yarn and
39 TCP. * indicates statistically difference for $p < 0.05$; **
40 indicates statistical difference for $p < 0.01$.

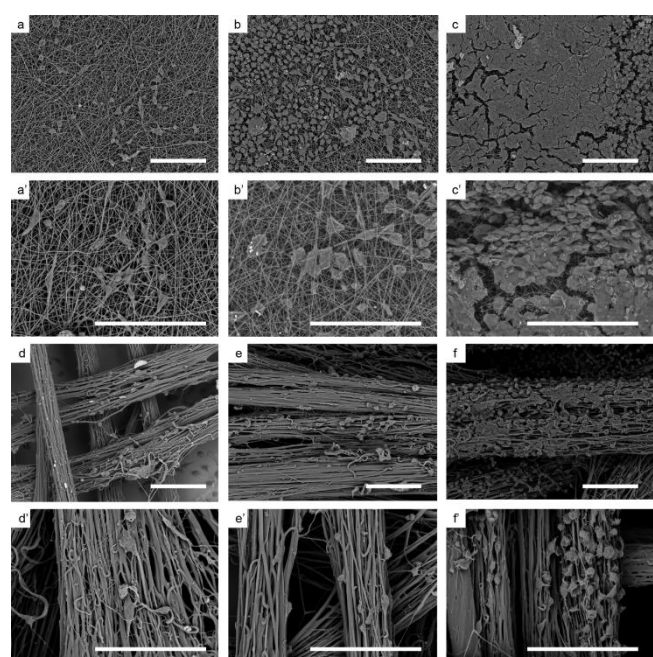
41 3.3 Cell morphology

42 The structure of scaffolds is the key issue for cell
43 colonization in tissue engineering. To study the
44 interaction between cells and different scaffolds, the
45 morphology of SCs on PLLA nanofiber yarn and film was
46 observed via SEM and CLSM images after 1, 3, 7 days of
47 culture. Fig. 4 and Fig. 5 illustrates the SEM images and
48 confocal microscopy of SCs, respectively. For the
49 confocal observation, the SCs were visualized by
50 staining the F-actin and nuclei into red and blue,
51 respectively.

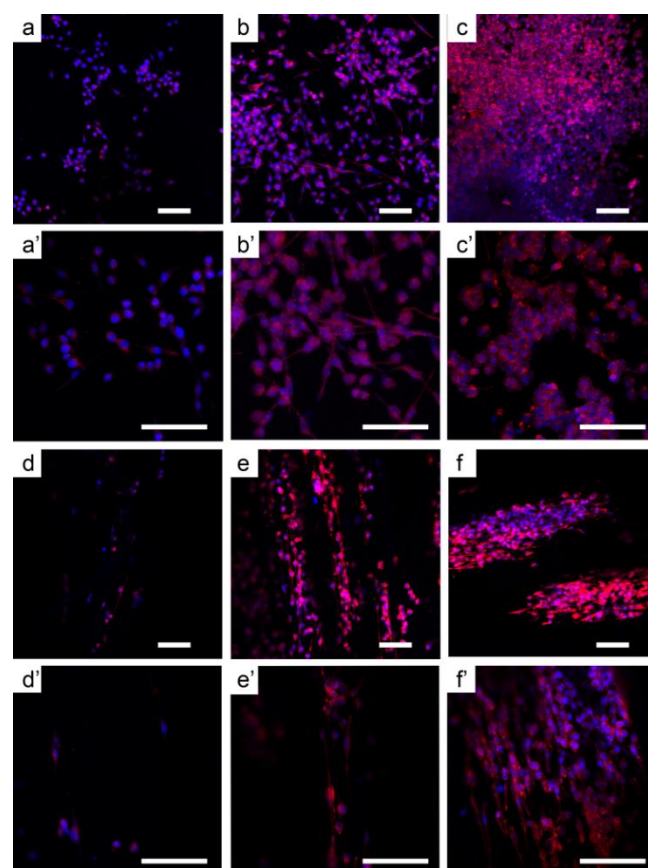
52 After 1 day of culture, polarized SCs are observed on
53 the nanofiber yarn with the long axis oriented in the
54 direction of yarn (Fig. 4 (d), (d')), while on the film,
55 randomly oriented cells of spindle or polygonal shapes
56 are observed (Fig. 4 (a), (a')). This phenomenon can be
57 confirmed by the confocal images in Fig. 5 (a), (a'), (d),
58 (d'). Longer axons of SCs can be clearly observed along
59 the nanofiber yarn (Fig. 5 (d)). These two different
60 phenotypes of SCs evidently observed on two scaffolds
61 become more obviously different in later culturing
62 period. After 3 days, more cells can be found on both
63 scaffolds (Fig. 4 (b), (e), Fig. 5 (b), (e)). Part of SCs
64 cultured on the film become spread-out, while the rest
65 cells are still randomly aligned across multiple fibers
66 and elongated along the fiber axes (Fig. 4 (b'), Fig. 5
67 (b')). In contrast, more SCs with long axons stretched
68 along the nanofiber yarn are observed (Fig. 4 (e), (e'),
69 Fig. 5 (e), (e')). The parallel red filaments indicates that
70 the aligned nanofiber induces cell extending
71 unidirectionally. 7 days after cell seeding, rounded
72 shaped SCs form a densely compacted layer and
73 occupied the whole surface of the film with no evident
74 axons observed (Fig. 4 (c), (c'), Fig. 5 (c), (c')). However,
75 the trend on nanofiber yarn keeps unchanged as the
76 number of SCs expands over time. More aligned SCs
77 surround the nanofiber yarn with only part of the
78 surface taken up, leaving sufficient space for further
79 cell migration and proliferation.

80 Previous studies have indicated that parallel nanofibers
81 determined the spreading and migration, as well as the
82 neurite outgrowth of nerve cells^{8, 19}. However, the
83 crossed fibers inhibited the further axonal extension of
84 SCs, which may be detrimental in the growth of
85 efficient and directed axons. Additionally, aligned fibers
86 also induced the differentiation and maturation of
87 neural stem cells and SCs^{25, 37}. Highly aligned nanofiber
88 scaffolds possessed the potential in nerve regeneration
89 for the cure of peripheral nerve injuries. Herein,
90 nanofiber yarn constructed by nanofibers highly
91 aligned along the axis of the yarn was fabricated via
92 dual needle electrospinning system. SCs were
93 cocultured with the yarn as well as film to assess axon
94 out growth and SCs behavior. SCs culture on the

1 showed a polarized structure along the axis of yarn,
 2 and the trend did not change over time during culture
 3 period. However, SCs on the film was randomly
 4 oriented with spread-out phenotype. As the time
 5 prolonged, SCs occupied the finite surface of the film
 6 and transformed into rounded shape. Without more
 7 space for cell spreading, the proliferation of SCs was
 8 inhibited and the outgrowth of axons was hindered. In
 9 contrary, the microscope structure constructed by the
 10 nanofiber yarn enlarged the effective space for cell
 11 migration and proliferation. Moreover, SCs on the
 12 nanofiber yarn could colonize in a three-dimensional
 13 space, which may be favorable for long time
 14 implantation and leave enough time for the
 15 regeneration of new nerve tissue in vivo.



16
 17 Fig. 4 SEM images of SCs on PLLA film and PLLA
 18 nanofiber yarn after cultured on PLLA film for 1 day(a),
 19 (a'), 3 days (b), (b'), 7 days (c), (c'), and PLLA nanofiber
 20 yarn for 1 day (d), (d'), 3 days (e), (e'), 7 days (f), (f'). (x)
 21 and (x') represent different magnification of 500 \times and
 22 2000 \times . (Double sided arrows indicated the yarn axis.
 23 Scale bar: 100 μ m.)



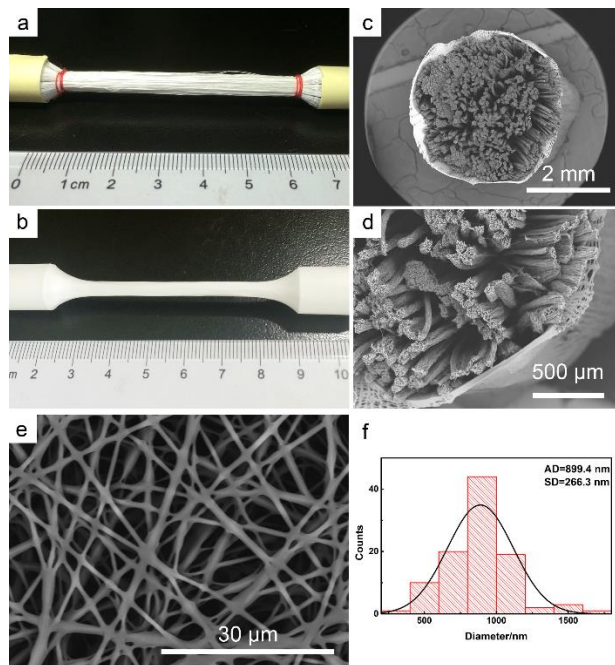
24
 25 Fig. 5 CLSM microscopy images of SCs on PLLA film and
 26 PLLA nanofiber yarn after cultured on PLLA film for 1
 27 day(a), (a'), 3 days (b), (b'), 7 days (c), (c'), and PLLA
 28 nanofiber yarn for 1 day (d), (d'), 3 days (e), (e'), 7 days
 29 (f), (f'). (x) and (x') represent different magnification of
 30 500 \times and 2000 \times . (Double sided arrows indicated the
 31 yarn axis. Scale bar: 100 μ m.)

32 3.4 Fabrication of nerve conduit with PLLA nanofiber 33 yarn

34 As manually inserting the nanofiber yarn into a hollow
 35 tube may cause additional curves and entanglements
 36 of yarns during operation, resulting in disordered
 37 structure in the lumen. The entangled yarn would
 38 mislead the spread and migration of cells in the conduit,
 39 consuming more time for the enclosure of the nerve
 40 deflection. To generate a uniform arrangement, the
 41 nanofiber yarn constructed by highly aligned nanofiber
 42 was incorporated into a nanofibrous conduit of P(LLA-
 43 CL) nanofiber as illustrated in Fig. 1 (g). PLLA yarns of
 44 two hundred are straightened and parallelly adhered
 45 around a metal stick as shown in Fig. 6 (a). After
 46 electrospinning P(LLA-CL) for 2 h, the surface of the
 47 yarn is covered with a thin layer of P(LLA-CL) nanofiber
 48 (Fig. 6 (b)), which can act as a barrier to limit the
 49 penetration of interstitial cells into the guide, as well as
 50 facilitate necessary suture while applied in clinic. After

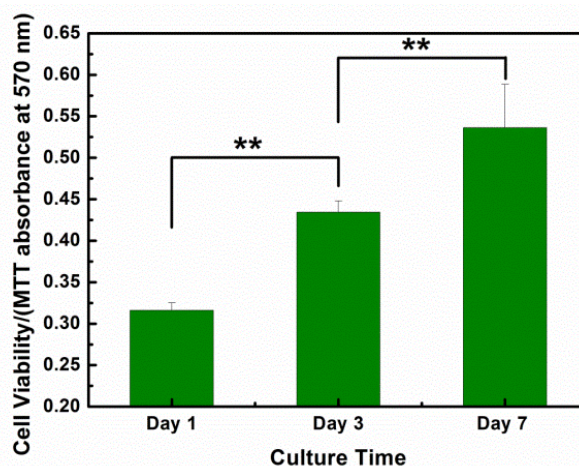
1 the removal of internal metal stick, a novel P(LLA-CL)
2 nerve conduit filled with PLLA nanofiber yarn is
3 obtained. The conduit was immersed into liquid
4 nitrogen and then cut into short sections for further
5 characterization. The radial cross section of the conduit
6 was observed by SEM and shown in Fig. 6 (c) and (d). It
7 can be seen that the yarns are parallelly inserted in the
8 lumen of the conduit with less curve and entanglement.
9 The inserted yarns can provide proper support and the
10 highly aligned nanofiber in the yarn can generate
11 topological guidance for cell migration and neurites
12 outgrowth across the nerve bridge. The SEM image of
13 the P(LLA-CL) layer is shown in Fig. 6 (e). The average
14 diameter of the P(LLA-CL) nanofiber is 899.4 ± 266.3 nm.

15 In addition, porosity in the lumen of conduit is a key
16 factor for nerve cell spreading, colonization,
17 proliferation, as well as new nerve tissue ingrowth.
18 Simply filling conduits with aligned fibers may block the
19 channels and hinder the infiltration and migration of
20 cells^{18, 21}. For this conduit, the porosity between yarns
21 left enough space for further cell migration. The
22 percentage of open region was determined by the
23 density of nanofiber yarns. For a given inner diameter
24 of conduit, the porosity increases while decrease the
25 number of nanofiber yarns inserted in. Thus the
26 porosity was controllable for a specific demand.



27
28 Fig. 6 Photo of the metal stick surrounded by PLLA
29 nanofiber yarn (a). Photo of nerve conduit after
30 electrospun P(LLA-CL) (b). SEM images of the cross
31 section of nerve conduit 30×(c), 100×(d). SEM image
32 (e) and diameter distribution (f) of the P(LLA-CL) layer.

33



34

35 Fig. 7 MTT assay of SCs cultured in the nerve conduit.

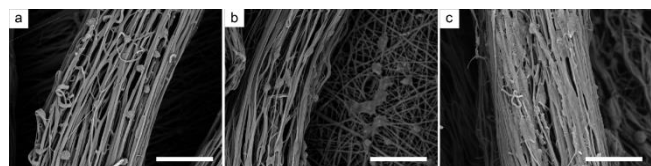
36 **3.5 SCs proliferation and migration in the conduit**

37 SCs were seeded in the nerve conduit sections with a
38 length of 9 mm by pipette a certain amount of SCs into
39 the lumen from one end of the conduit. The substrates
40 seeded with cells were placed in a shaker. The nutrition
41 and metabolic waste could only be transferred through
42 the P(LLA-CL) wall or the two ends of the conduit. As
43 illustrated in Fig.7, the MTT assay indicates that the
44 amount of SCs in the conduits go through slightly
45 increase during the 7 days of culture, indicating the
46 good biocompatibility of the nerve conduit. Obviously,
47 the increasing rate is much slower compared with
48 those cultured on PLLA nanofiber yarn (Fig. 3 (b)). This
49 can be attribute d to the methods of viability
50 determination. Part of the formazan form during MTT
51 incubation may not be dissolved by DMSO owing to the
52 barrier of P(LLA-CL) wall, resulting a relatively lower
53 absorbance.

54 Fig. 8 illustrates the morphology of SCs growing in the
55 conduit. The cultivated SCs show no visible difference
56 in appearance compared with those cultured on the
57 nanofiber yarn. On a single yarn, the amount of SCs
58 increases over culturing time. On the conduit wall of
59 P(LLA-CL), randomly oriented SCs are observed in Fig. 8
60 b.

61

62



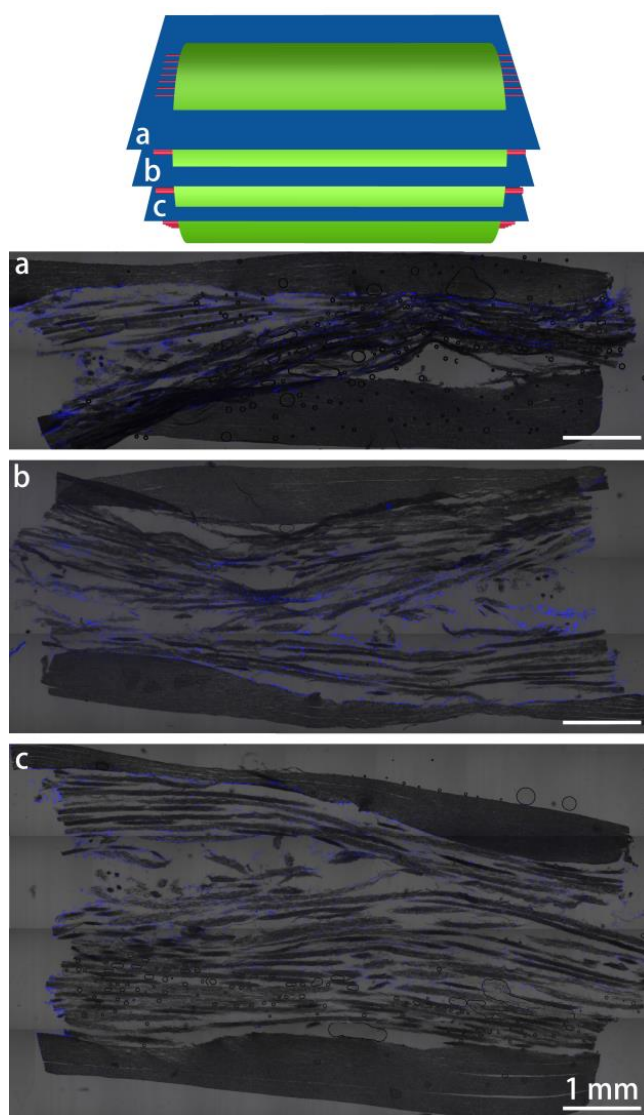
1
2 Fig. 8 SEM images of SCs cultured in the conduit
3 sections for 1 (a), 3 (b), and 7 days (c). (Scale bar: 50 μ m)

4 To determine the distribution of the SCs in the conduit,
5 cells were labeled by DAPI to generate blue
6 fluorescence and visualized by CLSM. Fig. 9
7 demonstrates the confocal microscopy photos of the
8 longitudinal section of nerve conduit combined with
9 SCs after 7 days of culture. SCs can be observed from
10 the wall (Fig. 9(a)) to the center of the conduit lumen
11 (Fig. 9 (a)). Moreover, across the longitudinal axis of the
12 conduit, the amount of SCs shows little difference,
13 indicating that SCs had migrated through the entire
14 lumen. According to the SEM images showed in Fig. 8
15 (c), after 7 days of culture, SCs have already covered
16 most surface of the nanofiber yarn, which made it
17 evident that the filling nanofiber yarn can positively
18 promote the spreading and migration of SCs in the
19 conduit.

20

21

22



23 Fig. 9 Longitudinal cross section of the nerve conduit
24 after coculturing with SCs for 7 days. (a), (b), and (c)
25 presented different levels of the conduit shown in the
26 schematic diagram.

27 Topological cues could significantly affect the behavior
28 of SCs including elongation, migration, alignment, as
29 well as subsequent axon extension. Previous study
30 indicated the size scale matters the alignment and
31 outgrowth of axons, which became significantly
32 improved while the fiber diameter was lowered down
33 from hundreds micrometer to hundreds nanometer^{38, 39}.
34 Electrospun fiber with a diameter ranging from tens
35 nanometer to several micrometer has drawn
36 considerable attention in the fabrication of nerve tissue
37 engineering scaffolds. Herein, PLLA nanofiber yarn with
38 highly aligned nanofiber was fabricated via dual
39 spinnerets electrospinning system. Parallel nanofiber
40 twisted into a bundle maintained the guidance cues as

1 the 2D film in addition of microscale structure and
2 feasibility for further processing. In vitro experiments
3 demonstrated that the PLLA nanofiber yarn scaffold
4 could promote SCs proliferation for its 3D structure and
5 high effective surface. The proliferating SCs could
6 express various ECM cell adhesion molecules and
7 plentiful growth promoting factors, enhancing the
8 further outgrowth of axons⁴⁰. The unidirectional
9 nanofiber in the surface also accelerated the
10 elongation and orientation of SCs and increased the
11 length of axons.

12 After injury of peripheral nerve, SCs proliferate,
13 reorganize, and align to form bands of Bungner¹⁹.
14 Nerve conduit is needed to bridge the lesion, providing
15 a guiding framework for the proliferation of neurons
16 and promote the related cells to generate inductive
17 factors for axonal outgrowth. Nanofiber filaments,
18 bundles, or 3D scaffolds with parallel nanofibers were
19 inserted in hollow tubes for enhanced cell alignment
20 and migration. However, the manual operation always
21 brought in entanglement of nanofibers and collapse of
22 the parallel structure, which would impede the growth
23 of regenerated nerve. Moreover, the structure of the
24 filaments, bundles, and 3D nanofibers was quite hard
25 to qualitatively control. In this study, we incorporated
26 the uniform PLLA nanofiber yarn consist of
27 longitudinally aligned nanofiber into a P(LLA-CL) tube to
28 fabricate a novel nerve conduit for peripheral nerve
29 regeneration. The PLLA nanofiber yarn distributed in a
30 3D configuration in the conduit, providing support for
31 cell adhesion and migration through the entire lumen,
32 while the aligned PLLA nanofiber guided the SCs growth
33 in a predetermined direction. In addition, the structure
34 of the conduit including conduit diameter and open
35 area could be adjusted to realize a specific design for
36 clinical demands.

37 In the present study, synthetic PLLA nanofiber yarn
38 could enhance the alignment, elongation of SCs and
39 outgrowth of axons. However, for further research, in
40 vivo experiment needs to be conducted to assess the
41 actual function of this novel conduit in nerve
42 regeneration. Natural materials of better
43 biocompatibility or the combination of natural and
44 synthetic materials could also be employed to
45 construct aligned yarn and conduit. Thus, quite a
46 number of materials and their combination could be
47 fabricated into nanofiber yarn to study the ability in
48 generating new nerve. Moreover, surface modified or
49 drug loaded nanofiber might be processed in the same
50 method to lead to better results in the repair of
51 peripheral nerve injuries.

52 Conclusion

53 In peripheral nerve injuries, nerve conduit bridges
54 between the broken stumps provides proper
55 configuration to facilitate support cell distribution and
56 the growth of injured nerve tissues in a predetermined
57 direction. Herein, a novel conduit was fabricated with
58 PLLA nanofiber yarn as the inner filler and P(LLA-CL)
59 nanofiber layer as the surrounding shell. In vitro
60 experiments indicated the good biocompatibility and
61 guiding capacity for spreading, migration, and
62 alignment of SCs. SCs cultured in the conduit section
63 migrated through the entire space in the conduit.
64 Based on the present data, it was believed that the
65 conduit possessed the ability for peripheral nerve
66 repair, which would be experimentally evaluated in
67 further studies.

68 Acknowledgements

69 This research was supported by National Natural
70 Science Foundation of China (31470941, 31271035, and
71 51403033), Science and Technology Commission of
72 Shanghai Municipality Program (14JC1492100,
73 15441905100), Ph.D. Programs Foundation of Ministry
74 of Education of China (20130075110005) and light of
75 textile project (J201404), the Fundamental Research
76 Funds for the Central Universities (CUSF-DH-D-
77 2014011and 2232014D3-15), and the Deanship of
78 Scientific Research at King Saud University for its
79 funding of this research through the research group
80 project no.RGP-201.

81 References

- 82
83 1. C. E. Schmidt and J. B. Leach, *Annual review of*
84 *biomedical engineering*, 2003, 5, 293-347.
85 2. J. H. Bell and J. W. Haycock, *Tissue engineering. Part*
86 *B, Reviews*, 2012, 18, 116-128.
87 3. J. Li, T. A. Rickett and R. Shi, *Langmuir*, 2008, 25,
88 1813-1817.
89 4. L. Yao, G. C. de Ruiter, H. Wang, A. M. Knight, R. J.
90 Spinner, M. J. Yaszemski, A. J. Windebank and A.
91 Pandit, *Biomaterials*, 2010, 31, 5789-5797.
92 5. F. Gelain, L. D. Unsworth and S. Zhang, *J. Controlled*
93 *Release*, 2010, 145, 231-239.
94 6. J. Xie, M. R. MacEwan, A. G. Schwartz and Y. Xia,
95 *Nanoscale*, 2010, 2, 35-44.
96 7. A. S. Hanna and R. Dempsey, *Neurosurgery*, 2010,
97 67, N14-N15.
98 8. H. B. Wang, M. E. Mullins, J. M. Cregg, C. W.
99 McCarthy and R. J. Gilbert, *Acta Biomater*, 2010, 6,
100 2970-2978.

- 1 9. T. Nakamura, Y. Inada, S. Fukuda, M. Yoshitani, A. Nakada, S. Itoi, S. Kanemaru, K. Endo and Y. Shimizu, *Brain Res*, 2004, 1027, 18-29.
- 2
3
4 10. D. Ceballos, X. Navarro, N. Dubey, G. Wendelschafer-Crabb, W. R. Kennedy and R. T. Tranquillo, *Experimental Neurology*, 1999, 158, 290-300.
- 5
6
7
8 11. T. Toba, T. Nakamura, Y. Shimizu, K. Matsumoto, K. Ohnishi, S. Fukuda, M. Yoshitani, H. Ueda, Y. Hori and K. Endo, *Journal of Biomedical Materials Research*, 2001, 58, 622-630.
- 9
10
11
12 12. F. Stang, H. Fansa, G. Wolf, M. Reppin and G. Keilhoff, *Biomaterials*, 2005, 26, 3083-3091.
- 13
14 13. S. Yoshii, S. Ito, M. Shima, A. Taniguchi and M. Akagi, *J Tissue Eng Regen Med*, 2009, 3, 19-25.
- 15
16 14. H. S. Koh, T. Yong, W. E. Teo, C. K. Chan, M. E. Puhaindran, T. C. Tan, A. Lim, B. H. Lim and S. Ramakrishna, *J Neural Eng*, 2010, 7, 046003.
- 17
18
19 15. B. S. Jha, R. J. Colello, J. R. Bowman, S. A. Sell, K. D. Lee, J. W. Bigbee, G. L. Bowlin, W. N. Chow, B. E. Mathern and D. G. Simpson, *Acta Biomater*, 2011, 7, 203-215.
- 20
21
22
23 16. M. F. Daud, K. C. Pawar, F. Claeysens, A. J. Ryan and J. W. Haycock, *Biomaterials*, 2012, 33, 5901-5913.
- 24
25
26 17. J. Cao, C. Sun, H. Zhao, Z. Xiao, B. Chen, J. Gao, T. Zheng, W. Wu, S. Wu, J. Wang and J. Dai, *Biomaterials*, 2011, 32, 3939-3948.
- 27
28
29 18. E. M. Jeffries and Y. Wang, *Biofabrication*, 2013, 5, 035015.
- 30
31 19. Y. T. Kim, V. K. Haftel, S. Kumar and R. V. Bellamkonda, *Biomaterials*, 2008, 29, 3117-3127.
- 32
33 20. C. Hinuber, K. Chwalek, F. J. Pan-Montojo, M. Nitschke, R. Vogel, H. Brunig, G. Heinrich and C. Werner, *Acta Biomater*, 2014, 10, 2086-2095.
- 34
35
36 21. A. Kriebel, M. Rumman, M. Scheld, D. Hodde, G. Brook and J. Mey, *Journal of biomedical materials research. Part B, Applied biomaterials*, 2014, 102, 356-365.
- 37
38
39
40 22. P. Sangsanoh, S. Waleetorncheepsawat, O. Suwantong, P. Wutticharoenmongkol, O. Weeranantanapan, B. Chuenjitbuntaworn, P. Cheepsunthorn, P. Pavasant and P. Supaphol, *Biomacromolecules*, 2007, 8, 1587-1594.
- 41
42
43
44
45 23. J. Xie, M. R. MacEwan, W. Liu, N. Jesuraj, X. Li, D. Hunter and Y. Xia, *ACS Appl Mater Interfaces*, 2014, 6, 9472-9480.
- 46
47
48 24. C. Huang, Y. Tang, X. Liu, A. Sutti, Q. Ke, X. Mo, X. Wang, Y. Morsi and T. Lin, *Soft Matter*, 2011, 7, 10812.
- 49
50
51 25. S. Y. Chew, R. Mi, A. Hoke and K. W. Leong, *Biomaterials*, 2008, 29, 653-661.
- 52
53 26. W. Martens, K. Sanen, M. Georgiou, T. Struys, A. Bronckaers, M. Ameloot, J. Phillips and I. Lambrechts, *FASEB journal : official publication of the Federation of American Societies for Experimental Biology*, 2014, 28, 1634-1643.
- 54
55
56
57
58 27. X. Gu, F. Ding, Y. Yang and J. Liu, *Progress in neurobiology*, 2011, 93, 204-230.
- 59
60 28. Y. Zhu, A. Wang, W. Shen, S. Patel, R. Zhang, W. Young and S. Li, *Adv Funct Mater*, 2010, 20, 1433-1440.
- 61
62
- 63 29. S. Y. Chew, R. Mi, A. Hoke and K. W. Leong, *Adv Funct Mater*, 2007, 17, 1288-1296.
- 64
65 30. F. Ko, Y. Gogotsi, A. Ali, N. Naguib, H. Ye, G. L. Yang, C. Li and P. Willis, *Adv. Mater.*, 2003, 15, 1161-1165.
- 66
67 31. E. Smit, U. Büttner and R. D. Sanderson, *Polymer*, 2005, 46, 2419-2423.
- 68
69 32. W.-E. Teo, R. Gopal, R. Ramaseshan, K. Fujihara and S. Ramakrishna, *Polymer*, 2007, 48, 3400-3405.
- 70
71 33. X. Wang, K. Zhang, M. Zhu, H. Yu, Z. Zhou, Y. Chen and B. S. Hsiao, *Polymer*, 2008, 49, 2755-2761.
- 72
73 34. M. S. M. Jad, S. A. H. Ravandi, H. Tavanai and R. H. Sanatgar, *Fibers Polym.*, 2011, 12, 801-807.
- 74
75 35. H. Yan, L. Liu and Z. Zhang, *Mater. Lett.*, 2011, 65, 2419-2421.
- 76
77 36. U. Ali, Y. Zhou, X. Wang and T. Lin, *J. Text. Inst.*, 2012, 103, 80-88.
- 78
79 37. L. He, S. Liao, D. Quan, K. Ma, C. Chan, S. Ramakrishna and J. Lu, *Acta Biomater*, 2010, 6, 2960-2969.
- 80
81
82 38. X. Wen and P. A. Tresco, *Journal of biomedical materials research. Part A*, 2006, 76, 626-637.
- 83
84 39. F. Yang, R. Murugan, S. Wang and S. Ramakrishna, *Biomaterials*, 2005, 26, 2603-2610.
- 85
86 40. S. Madduri, M. Papaloizos and B. Gander, *Biomaterials*, 2010, 31, 2323-2334.
- 87
- 88

Abstract

PLLA was electrospun into nanofiber yarn, which was then covered by P(LLA-CL) nanofiber tube to form a nerve conduit. PLLA nanofiber yarn as the inner filler and P(LLA-CL) nanofiber film as the surrounding shell. In vitro experiments indicated the good biocompatibility and guiding capacity for spreading, migration, and alignment of SCs.

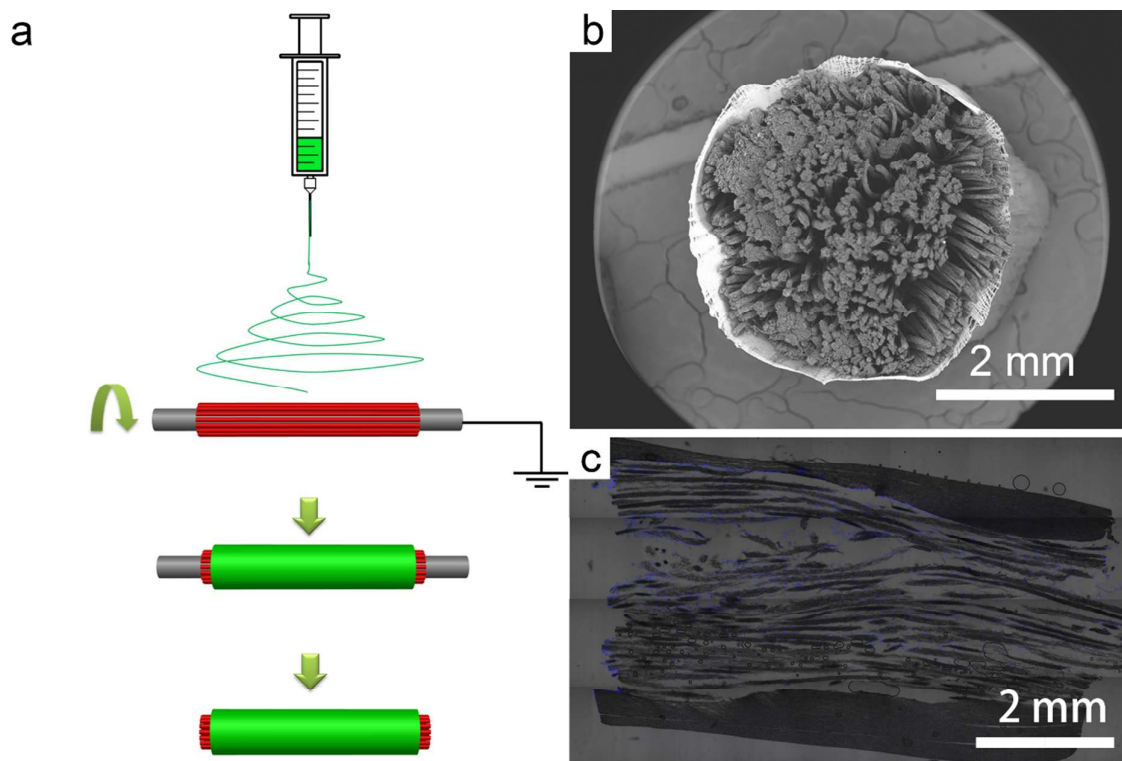


Fig (a) Schematic of incorporating nanofiber yarn into the conduit. (b) SEM image of the crosssection of nerve conduit after electrospun P(LLA-CL). (c) Longitudinal cross section of the nerve conduit after coculturing with SCs for 7 days.